Evaluation of two-photon exchange graphs for highly charged heliumlike ions

Steven A. Blundell
Département de Recherche Fondamentale, LI2A, Centre d'Etudes Nucléaires de Grenoble, Boîte Postale 85X, F-38041 Grenoble Cedex, France

Peter J. Mohr
National Institute of Standards and Technology, Gaithersburg, Maryland 20899

W. R. Johnson and J. Sapirstein
Department of Physics, University of Notre Dame, Notre Dame, Indiana 46556
(Received 4 June 1993)

Contributions of one-loop ladder and crossed-ladder graphs to the ground-state energy of heliumlike ions are calculated in Furry representation QED. With the aid of a contour rotation, the graphs are evaluated to all orders in $Z\alpha$ in the range $Z = 10$–110. Particular attention is given to the relation of this work to recent many-body perturbation theory and configuration-interaction calculations.

PACS number(s): 12.20.Ds, 31.20.Tz, 31.30.Jv

I. INTRODUCTION

Relativistic many-body perturbation theory (MBPT) has been shown to lead to rapidly convergent solutions to the many-electron Dirac equation for highly charged heliumlike [1] and alkali-metal-like [2] ions. An important component of these calculations is the second-order energy $E^{(2)}$ which involves a double sum over intermediate states. In the relativistic case, the treatment of intermediate negative-energy states is problematical. This can be illustrated for the case of ground-state heliumlike ions, where the second-order energy is given by

$$E^{(2)} = \sum_{\substack{i,j \\ (i,j)\neq(a,b)}} \frac{g_{abij}g_{ijab} - g_{abij}g_{ijba}}{2\epsilon_a - \epsilon_i - \epsilon_j}\,, \tag{1.1}$$

when the electron-electron interaction is the perturbation. In Eq. (1.1), the Coulomb matrix element g_{ijkl} is defined by

$$g_{ijkl} = \int d\mathbf{x}_2 d\mathbf{x}_1 \psi_i^\dagger(\mathbf{x}_2)\psi_k(\mathbf{x}_2)\frac{\alpha}{|\mathbf{x}_2 - \mathbf{x}_1|}\psi_j^\dagger(\mathbf{x}_1)\psi_l(\mathbf{x}_1)\,, \tag{1.2}$$

and a and b represent the two occupied $1s$ states with spin projections $m = \pm 1/2$. If the states i and j are allowed to range freely over both positive- and negative-energy states, vanishing energy denominators can result when one is positive and the other negative. This is related to the well-known *continuum dissolution* problem [3]. In practical calculations this problem is solved by summing over positive-energy states only, or equivalently, using the "no-pair" Hamiltonian [3] in which only the positive-energy components of one- and two-particle operators appear. The effects of negative-energy states do, however, enter as radiative corrections. To evaluate these corrections, a field theoretic approach must be taken.

There are a number of ways to treat helium starting from QED. The earliest treatment following the development of modern QED was by Brown and Ravenhall [4]. This work was primarily concerned with justifying the older Breit equation [5], which gave the correct fine structure of helium only after an *ad hoc* rule was imposed on perturbation theory. Brown and Ravenhall made a contact transformation on the QED wave function that eliminated the transverse part of the QED Hamiltonian in lowest approximation. Transforming the resulting Schrödinger equation to configuration space led to a well-defined Hamiltonian problem with projection operators; essentially the no-pair Hamiltonian. In higher orders, multiple commutators give rise to the Breit interaction and QED effects, the latter of which were shown to enter in order α^3 a.u., though they were not explicitly calculated in [4]. The Brown-Ravenhall contact transformation was later discussed by Mittleman [6] and applied to a three-body problem by Zygelman and Mittleman [7].

Following the work of Brown and Ravenhall, further progress was made in the framework of the Bethe-Salpeter (BS) equation [8]. In this method, the poles of the electron-electron scattering Green's function in an external nuclear Coulomb field are analyzed. The BS equation was applied to neutral helium by Sucher [9], Araki [10], Kabir and Salpeter [11], and Douglas and Kroll [12] with considerable success. However, nonrelativistic approximations are made in several parts of these calculations, so that the validity of applying the BS approach to highly charged ions is questionable. In order to avoid the need for nonrelativistic approximations, we use the S-matrix technique [13] here, in which the symmetric form of the Gell-Mann and Low formula [14], introduced by Sucher [15], relates energy levels to Feynman diagrams.

While this method in practice can be applied only to low-order Feynman diagrams, as opposed to the infinite set of ladder diagrams automatically included in Bethe-Salpeter approaches, the $1/Z$ expansion [16] ensures that higher order diagrams are suppressed by powers of $1/Z$, so that consideration of only a small number of Feynman diagrams allows precise predictions for the spectra of highly charged ions. In addition, ions with more than two electrons can be treated using similar methods.

The S-matrix approach has been applied through second order, in which case the only Feynman diagrams are those shown in Fig. 1. While the evaluation of the graph of Fig. 1(a), where a photon is exchanged between two electrons, is straightforward [13], the self-energy and vacuum polarization diagrams of Figs. 1(b) and 1(c), respectively, present a more challenging numerical problem that has received considerable attention recently [17]. Applications through fourth order, by contrast, have not yet been carried out. There are four types of fourth-order diagram shown in Fig. 2. The second-order energy from MBPT is associated with the diagrams of Figs. 2(a) and 2(b), which we refer to as the ladder (L) and crossed ladder (X), respectively. It is these diagrams that will be calculated in this paper. The remaining diagrams will not be treated here, but will be discussed in the conclusion.

While the ladder and crossed-ladder diagrams will be evaluated from QED here, it is important to discuss their relation to MBPT calculations. This is because of recent progress in the solution of the no-pair Hamiltonian problem with MBPT [1] and configuration-interaction calculations [18]. By using large relativistic basis sets with negative-energy states excluded, high-accuracy solutions to the energy levels of ground state and $n = 2$ excited states of helium incorporating the instantaneous Breit interaction are now available. However, QED effects must also be included, and it is important to include them in a consistent way. Thus we must separate from our present calculation those terms already included in the solution to the no-pair Hamiltonian. While we have carried out our analysis in both Feynman and Coulomb gauges, the connection to MBPT is most clearly seen in Coulomb gauge. In this gauge, the photon propagators have two parts, an instantaneous Coulomb interaction (C) and a retarded magnetic or transverse interaction (B). When both photons are type (C), a simple analysis [19] shows

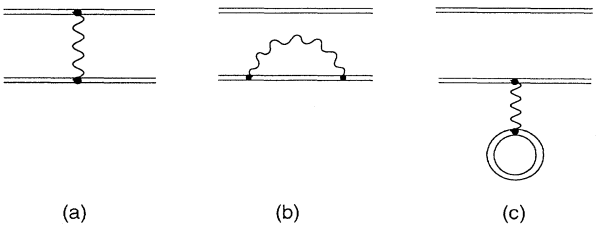

FIG. 1. Second-order Feynman diagrams contributing to the energy of heliumlike ions.

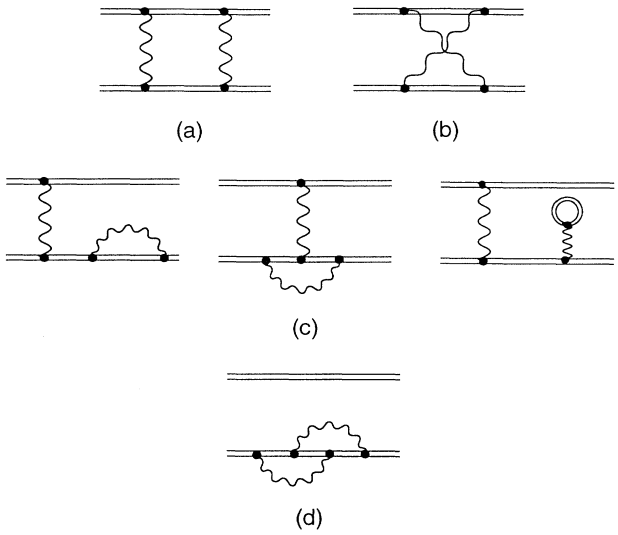

FIG. 2. Fourth-order Feynman diagrams contributing to the energy of heliumlike ions. (a) Ladder diagram, (b) crossed-ladder diagram, (c) sample diagrams involving one radiative correction and one additional exchanged photon, (d) example of a two-loop radiative correction.

that the part of Eq. (1.1) with i and j both positive-energy states is exactly reproduced. Further, the terms associated with continuum dissolution vanish and there remains only a small radiative correction term in which i and j are both negative-energy states. This last term can be shown (at low Z) to enter in order $(Z\alpha)^3$ a.u. [19]; it is one of a set of terms entering in this order that were evaluated in the Bethe-Salpeter approach discussed above. When one photon is type (C) and the other type (B), the same analysis leads (in the approximation that the transverse photon exchange is instantaneous) to an important MBPT contribution referred to here as the "Breit-Coulomb" term $B^{(2)}$ which enters in order $(Z\alpha)^2$ a.u. and is part of the fine structure. Again, corrections to this term enter in order $(Z\alpha)^3$ a.u.. Finally, when both photons are transverse, the same approximation gives a term that we refer to as the "Breit-Breit" term, B-B, which is also of leading order $(Z\alpha)^3$ a.u., and which has only recently been evaluated. Another feature of note is the importance of the contribution with two negative-energy intermediate states because of the relative enhancement of $\boldsymbol{\alpha}$ between a positive- and negative-energy state. The retardation factor plays an important role here, as dropping it leads to an incorrect contribution of order of fine structure. The actual contribution is of order $(Z\alpha)^3 \ln Z\alpha$.

The general situation that we have just described is that the ladder and crossed-ladder diagrams contain some important MBPT effects, but in addition contain field theoretic effects beginning in order $(Z\alpha)^3$. Because we are interested in highly charged ions, we want to evaluate these diagrams without assuming $Z\alpha \ll 1$. To do this, we now turn to the exact QED calculation. Fol-

lowing this, in Sec. III, we separate out the MBPT parts of the calculation, and compare with the known $(Z\alpha)^3$ results. This will allow us to infer the QED corrections to the MBPT calculations. Finally, in Sec. IV, the role of the other QED diagrams and prospects for future progress will be discussed.

II. FORMULATION

In the S-matrix approach, the fourth-order energy is

$$E^{(4)} = \lim_{\epsilon\to 0} \frac{i\epsilon}{2}[4\langle S_\epsilon^{(4)}\rangle_c - 2\langle S_\epsilon^{(2)}\rangle_c^2] , \tag{2.1}$$

where

$$\langle S_\epsilon^{(4)}\rangle_c = \frac{(-i)^4}{4!}\int d^4x_4\int d^4x_3\int d^4x_2\int d^4x_1\; e^{-\epsilon(|t_4|+|t_3|+|t_2|+|t_1|)}\langle T\,[H_I(x_4)H_I(x_3)H_I(x_2)H_I(x_1)]\rangle_c \tag{2.2}$$

and

$$\langle S_\epsilon^{(2)}\rangle_c = \frac{(-i)^2}{2!}\int d^4x_2\int d^4x_1\; e^{-\epsilon(|t_2|+|t_1|)}\langle T\,[H_I(x_2)H_I(x_1)]\rangle_c\,. \tag{2.3}$$

Here

$$H_I(x) = -j_\mu(x)\,A^\mu(x)\,, \tag{2.4}$$

where $j_\mu(x)$ is the electron-positron current, $A^\mu(x)$ is the quantized radiation field, and T is the time ordering operator.

We now consider the terms from two contractions in $S_\epsilon^{(4)}$, corresponding to the Feynman diagrams of Fig. 2(a), the ladder (L),

$$\begin{aligned}\langle S_\epsilon^{(4)}\rangle_L = \frac{e^4}{2}\int d^4x_4\int d^4x_3\int d^4x_2\int d^4x_1\; e^{-\epsilon(|t_4|+|t_3|+|t_2|+|t_1|)}\sum_{n_4,n_3,n_2,n_1}\langle a^\dagger_{n_4}a^\dagger_{n_2}a_{n_1}a_{n_3}\rangle\\ \times\bar\phi_{n_4}(x_4)\gamma_\mu S_F(x_4,x_3)\gamma_\nu\phi_{n_3}(x_3)\bar\phi_{n_2}(x_2)\gamma^\mu S_F(x_2,x_1)\gamma^\nu\phi_{n_1}(x_1)\\ \times D_F(x_4-x_2)D_F(x_3-x_1)\end{aligned} \tag{2.5}$$

and Fig. 2(b), the crossed ladder (X)

$$\begin{aligned}\langle S_\epsilon^{(4)}\rangle_X = \frac{e^4}{2}\int d^4x_4\int d^4x_3\int d^4x_2\int d^4x_1\; e^{-\epsilon(|t_4|+|t_3|+|t_2|+|t_1|)}\sum_{n_4,n_3,n_2,n_1}\langle a^\dagger_{n_4}a^\dagger_{n_2}a_{n_1}a_{n_3}\rangle\\ \times\bar\phi_{n_4}(x_4)\gamma_\mu S_F(x_4,x_3)\gamma_\nu\phi_{n_3}(x_3)\bar\phi_{n_2}(x_2)\gamma^\nu S_F(x_2,x_1)\gamma^\mu\phi_{n_1}(x_1)\\ \times D_F(x_4-x_1)D_F(x_3-x_2).\end{aligned} \tag{2.6}$$

While we present these expressions in Feynman gauge, we carry out the actual numerical calculations in Coulomb gauge as well, finding numerically that their sum is gauge invariant.

In Eqs. (2.5) and (2.6), $S_F(x_2,x_1)$ is the bound electron propagation function given by

$$\begin{aligned}S_F(x_2,x_1) &= \langle 0|T[\psi(x_2)\bar\psi(x_1)]|0\rangle\\ &= \frac{1}{2\pi i}\int_{-\infty}^{\infty}dz\sum_n\frac{\phi_n(\mathbf{x}_2)\bar\phi_n(\mathbf{x}_1)}{E_n - z(1+i\delta)}\;e^{-iz(t_2-t_1)}\\ &= \frac{1}{2\pi i}\int_{-\infty}^{\infty}dz\;G\big(\mathbf{x}_2,\mathbf{x}_1,z(1+i\delta)\big)\gamma^0\\ &\quad\times e^{-iz(t_2-t_1)},\end{aligned} \tag{2.7}$$

where $G(\mathbf{x}_2,\mathbf{x}_1,z)$ is the Green's function for the Dirac equation

$$[-i\boldsymbol{\alpha}\cdot\boldsymbol{\nabla}_2 + V(\mathbf{x}_2) + \beta - z]\,G(\mathbf{x}_2,\mathbf{x}_1,z) = \delta(\mathbf{x}_2-\mathbf{x}_1). \tag{2.8}$$

The function $D_F(x_2-x_1)$ is proportional to the Feynman gauge photon propagation function, which is given by

$$g_{\mu\nu}D_F(x_2-x_1) = \langle 0|T\,[A_\mu(x_2)A_\nu(x_1)]\,|0\rangle. \tag{2.9}$$

Here

$$\begin{aligned}D_F(x_2-x_1) &= -\frac{i}{(2\pi)^4}\int d^4q\frac{e^{-iq(x_2-x_1)}}{q^2+i\delta}\\ &= \frac{1}{2\pi i}\int_{-\infty}^{\infty}dq_0\;H(\mathbf{x}_2-\mathbf{x}_1,q_0)e^{-iq_0(t_2-t_1)}\end{aligned} \tag{2.10}$$

and

$$H(\mathbf{x}_2-\mathbf{x}_1,q_0) = -\frac{e^{-bx_{21}}}{4\pi x_{21}}$$
$$x_{21} = |\mathbf{x}_2-\mathbf{x}_1|\;;\; b = -i(q_0^2+i\delta)^{1/2}\;,\;\mathrm{Re}(b)>0. \tag{2.11}$$

The time dependence of the wave functions is given by $\phi_n(\mathbf{x})e^{-iE_nt}$. Substituting (2.7) and (2.10) into (2.5) and (2.6), and carrying out the integration over time variables yields

$$\langle S_\epsilon^{(4)}\rangle_L = \frac{8\alpha^2}{\pi^2}\int d\mathbf{x}_4\int d\mathbf{x}_3\int d\mathbf{x}_2\int d\mathbf{x}_1 \times\int_{-\infty}^{\infty}dq_2\int_{-\infty}^{\infty}dq_1\int_{-\infty}^{\infty}dz_2\int_{-\infty}^{\infty}dz_1\sum_{n_4,n_3,n_2,n_1}\langle a_{n_4}^\dagger a_{n_2}^\dagger a_{n_1}a_{n_3}\rangle \times\frac{\epsilon}{\epsilon^2+(E_{n_4}-z_2-q_2)^2}\,\frac{\epsilon}{\epsilon^2+(E_{n_3}-z_2+q_1)^2} \times\frac{\epsilon}{\epsilon^2+(E_{n_2}-z_1+q_2)^2}\,\frac{\epsilon}{\epsilon^2+(E_{n_1}-z_1-q_1)^2} \times\phi_{n_4}^\dagger(\mathbf{x}_4)\alpha_\mu G(\mathbf{x}_4,\mathbf{x}_3,z_2(1+i\delta))\alpha_\nu\phi_{n_3}(\mathbf{x}_3)H(\mathbf{x}_4-\mathbf{x}_2,q_2) \times\phi_{n_2}^\dagger(\mathbf{x}_2)\alpha^\mu G(\mathbf{x}_2,\mathbf{x}_1,z_1(1+i\delta))\alpha^\nu\phi_{n_1}(\mathbf{x}_1)H(\mathbf{x}_3-\mathbf{x}_1,q_1) \tag{2.12}$$

and

$$\langle S_\epsilon^{(4)}\rangle_X = \frac{8\alpha^2}{\pi^2}\int d\mathbf{x}_4\int d\mathbf{x}_3\int d\mathbf{x}_2\int d\mathbf{x}_1 \times\int_{-\infty}^{\infty}dq_2\int_{-\infty}^{\infty}dq_1\int_{-\infty}^{\infty}dz_2\int_{-\infty}^{\infty}dz_1\sum_{n_4,n_3,n_2,n_1}\langle a_{n_4}^\dagger a_{n_2}^\dagger a_{n_1}a_{n_3}\rangle \times\frac{\epsilon}{\epsilon^2+(E_{n_4}-z_2-q_2)^2}\,\frac{\epsilon}{\epsilon^2+(E_{n_3}-z_2+q_1)^2} \times\frac{\epsilon}{\epsilon^2+(E_{n_2}-z_1+q_1)^2}\,\frac{\epsilon}{\epsilon^2+(E_{n_1}-z_1-q_2)^2} \times\phi_{n_4}^\dagger(\mathbf{x}_4)\alpha_\mu G(\mathbf{x}_4,\mathbf{x}_3,z_2(1+i\delta))\alpha_\nu\phi_{n_3}(\mathbf{x}_3)H(\mathbf{x}_4-\mathbf{x}_1,q_2) \times\phi_{n_2}^\dagger(\mathbf{x}_2)\alpha^\nu G(\mathbf{x}_2,\mathbf{x}_1,z_1(1+i\delta))\alpha^\mu\phi_{n_1}(\mathbf{x}_1)H(\mathbf{x}_3-\mathbf{x}_2,q_1)\,. \tag{2.13}$$

It is convenient at this point to define the Feynman gauge generalization of Eq. (1.2),

$$g_{ijkl}(q) = -4\pi\alpha\int d\mathbf{x}_2\int d\mathbf{x}_1 H(\mathbf{x}_2-\mathbf{x}_1,q)\phi_i^\dagger(\mathbf{x}_2) \times\alpha_\mu\phi_k(\mathbf{x}_2)\phi_j^\dagger(\mathbf{x}_1)\alpha^\mu\phi_l(\mathbf{x}_1)\,. \tag{2.14}$$

We do this because we will now replace $G(\mathbf{x}_i,\mathbf{x}_j,z(1+i\delta))$ by its spectral decomposition on the second line of Eq. (2.7). This allows us to reexpress Eqs. (2.12) and (2.13) in terms of products of g_{ijkl} factors. These two equations are valid for any state of a two-electron ion, but the following discussion is specialized to the $^1S_0$ ground state:

$$|1s^2\ {}^1S_0\rangle = a_b^\dagger a_a^\dagger|0\rangle\,, \tag{2.15}$$

for which

$$E_{n_4}=E_{n_3}=E_{n_2}=E_{n_1}=E_0, \tag{2.16}$$

and where the replacement

$$\sum_{n_4,n_3,n_2,n_1}\langle a_{n_4}^\dagger a_{n_2}^\dagger a_{n_1}a_{n_3}\rangle f(n_4,n_3,n_2,n_1) = 2[f(a,a,b,b)-f(a,b,b,a)], \tag{2.17}$$

that takes into account the spherical symmetry of the interaction: $g_{a,b,c,d}(q)=g_{-a,-b,-c,-d}(q)$, can be made. For this special case we may write Eqs. (2.12) and (2.13) as

$$\langle S_\epsilon^{(4)}\rangle_L = \frac{1}{\pi^4}\int_{-\infty}^{\infty}dq_2\int_{-\infty}^{\infty}dq_1\sum_{n,m}[g_{abnm}(q_2)g_{nmab}(q_1)-g_{abnm}(q_2)g_{nmba}(q_1)] \times\int_{-\infty}^{\infty}dz_2\int_{-\infty}^{\infty}dz_1\frac{1}{E_n-z_2(1+i\delta)}\,\frac{\epsilon}{\epsilon^2+(E_0-z_2-q_2)^2} \times\frac{\epsilon}{\epsilon^2+(E_0-z_2+q_1)^2}\,\frac{1}{E_m-z_1(1+i\delta)} \times\frac{\epsilon}{\epsilon^2+(E_0-z_1+q_2)^2}\,\frac{\epsilon}{\epsilon^2+(E_0-z_1-q_1)^2} \tag{2.18}$$

and

$$\langle S_\epsilon^{(4)}\rangle_X = \frac{1}{\pi^4}\int_{-\infty}^{\infty} dq_2 \int_{-\infty}^{\infty} dq_1 \sum_{n,m}[g_{amnb}(q_2)g_{bnma}(q_1) - g_{amna}(q_2)g_{bnmb}(q_1)]$$
$$\times \int_{-\infty}^{\infty} dz_2 \int_{-\infty}^{\infty} dz_1 \frac{1}{E_n - z_2(1+i\delta)} \frac{\epsilon}{\epsilon^2 + (E_0 - z_2 - q_2)^2}$$
$$\times \frac{\epsilon}{\epsilon^2 + (E_0 - z_2 + q_1)^2} \frac{1}{E_m - z_1(1+i\delta)}$$
$$\times \frac{\epsilon}{\epsilon^2 + (E_0 - z_1 + q_1)^2} \frac{\epsilon}{\epsilon^2 + (E_0 - z_1 - q_2)^2}\,. \tag{2.19}$$

The corresponding second-order exchanged-photon term (E) is

$$\langle S_\epsilon^{(2)}\rangle_E = -\frac{e^2}{2}\int d^4x_2 \int d^4x_1\, e^{-\epsilon(|t_2|+|t_1|)} \sum_{n_4,n_3,n_2,n_1} \langle a^\dagger_{n_4} a^\dagger_{n_2} a_{n_1} a_{n_3}\rangle$$
$$\times \bar\phi_{n_4}(x_2)\gamma_\mu\phi_{n_3}(x_2)\bar\phi_{n_2}(x_1)\gamma^\mu\phi_{n_1}(x_1)D_F(x_2 - x_1)$$
$$= -\frac{2i}{\pi}\int_{-\infty}^{\infty} dq\,[g_{abab}(q) - g_{abba}(q)]\frac{\epsilon^2}{(\epsilon^2+q^2)^2}\,. \tag{2.20}$$

A. Excited intermediate states

For small ϵ, the dominant contribution to the integrals in Eqs. (2.18) and (2.19) comes from the region $q_2 \approx E_0 - z_2$ and $q_1 \approx z_2 - E_0$. When at least one intermediate state is excited, it is sufficient to consider the leading term in a power series expansion of the photon functions H about these points to evaluate the leading contribution to the matrix elements in powers of ϵ [20]. In the first term from such an expansion, integration over q_2 and q_1 and the translations $z_2 \to z_2 + E_0$ and $z_1 \to z_1 + E_0$ yield

$$\langle S_\epsilon^{(4)}\rangle_L = \frac{1}{\pi^4}\int_{-\infty}^{\infty} dz_2 \int_{-\infty}^{\infty} dz_1 \sum_{n,m}[g_{abnm}(z_2)g_{nmab}(z_2) - g_{abnm}(z_2)g_{nmba}(z_2)]$$
$$\times \frac{1}{E_n - (z_2+E_0)(1+i\delta)} \frac{1}{E_m - (z_1+E_0)(1+i\delta)} \left[\frac{2\pi\epsilon}{4\epsilon^2 + (z_2+z_1)^2}\right]^2, \tag{2.21}$$

and

$$\langle S_\epsilon^{(4)}\rangle_X = \frac{1}{\pi^4}\int_{-\infty}^{\infty} dz_2 \int_{-\infty}^{\infty} dz_1 \sum_{n,m}[g_{amnb}(z_2)g_{bnma}(z_2) - g_{amna}(z_2)g_{bnmb}(z_2)]$$
$$\times \frac{1}{E_n - (z_2+E_0)(1+i\delta)} \frac{1}{E_m - (z_1+E_0)(1+i\delta)} \left[\frac{2\pi\epsilon}{4\epsilon^2 + (z_2+z_1)^2}\right]^2. \tag{2.22}$$

If $E_m \neq E_0$ or $E_n \neq E_0$, the integration over z_1 can be carried out, and then application of Eq. (2.1) gives the energy shifts

$$\Delta E_L = \frac{i}{4\pi}\sum_{a,b,n,m}\int_{-\infty}^{\infty} dz \frac{g_{mnab}(z)\tilde g_{abmn}(z)}{[E_a - z - E_m(1-i\delta)][E_a + z - E_n(1-i\delta)]}\,, \tag{2.23}$$

$$\Delta E_X = \frac{i}{4\pi}\sum_{a,b,n,m}\int_{-\infty}^{\infty} dz \frac{g_{anmb}(z)g_{bmna}(z) - g_{anma}(z)g_{bmnb}(z)}{[E_a + z - E_n(1-i\delta)][E_a + z - E_m(1-i\delta)]}\,, \tag{2.24}$$

where $\tilde{g}_{ijkl} \equiv g_{ijkl} - g_{ijlk}$. Here the sum over a and b is over magnetic substates of the $1s$ state, and was introduced, with a compensating factor of $1/2$, to facilitate the angular reduction of the terms.

We have also analyzed the corrections to this from the expansion of the photon propagators, and shown that they vanish. We show in Fig. 3 the poles and cuts in the complex z plane associated with the electron and photon propagators. In the absence of cuts, the z integration can be carried out with Cauchy's theorem, and MBPT-like formulas obtained. However, we choose here to make the contour rotation indicated in Fig. 3. When one intermediate state is $1s$ and the other not, the contour includes a semicircle around a pole at $z = 0$, which gives the contributions

$$\Delta E_L^{\rm pole} = \frac{1}{2} \sum_{\substack{a,b,c,m \\ (m \neq a)}} \frac{g_{abcm}(0)\tilde{g}_{cmab}(0)}{E_a - E_m} \tag{2.25}$$

and

$$\Delta E_X^{\rm pole} = \frac{1}{2} \sum_{\substack{a,b,c,m \\ (m \neq a)}} \frac{g_{bmca}(0)g_{cabm}(0) - g_{amca}(0)g_{cbbm}(0)}{E_a - E_m} . \tag{2.26}$$

Note that the sum over m includes both negative- and positive-energy states. For the rest of the contour, the change of variable $z \to i\omega$ then leads to

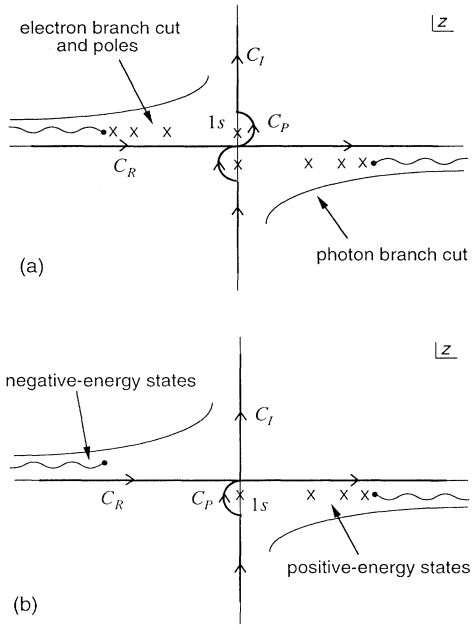

FIG. 3. Singularities of the integrand of (a) ΔE_L and (b) ΔE_X in the complex z plane. The contour C_R is rotated anticlockwise about $z = 0$ to give C_I plus half-pole terms C_P.

$$\Delta E_{CL} = -\frac{1}{2\pi} \sum_{a,b,m,n} \int_0^\infty d\omega \frac{\omega^2 + X_m Y_n}{(\omega^2 + X_m^2)(\omega^2 + Y_n^2)} g_{mnab}(i\omega)\tilde{g}_{abmn}(i\omega) \tag{2.27}$$

and

$$\Delta E_{CX} = -\frac{1}{2\pi} \sum_{a,b,m,n} \int_0^\infty d\omega \frac{-\omega^2 + X_m Y_n}{(\omega^2 + X_m^2)(\omega^2 + Y_n^2)} [g_{anmb}(i\omega)g_{bmna}(i\omega) - g_{anma}(i\omega)g_{bmnb}(i\omega)] , \tag{2.28}$$

where $X_m \equiv E_a - E_m$ and $Y_n \equiv E_b - E_n$. The evaluation of the expressions (2.27) and (2.28) constitutes the main numerical work in the present calculation.

B. Degenerate intermediate states

We next consider Eqs. (2.18) and (2.19) for intermediate states that are degenerate with the ground state, i.e., $E_n = E_m = E_0$. In this case, $\langle S_\epsilon^{(4)} \rangle_L$ contains a singularity of order ϵ^{-2} that cancels a similar term in $\langle S_\epsilon^{(2)} \rangle_E^2$, and there is a finite remainder that is discussed in this section. In particular, we have

$$\langle S_\epsilon^{(4)} \rangle_L = \frac{1}{\pi^4} \int_{-\infty}^\infty dq_2 \int_{-\infty}^\infty dq_1 \sum_{c,d} [g_{abcd}(q_2)g_{cdab}(q_1) - g_{abcd}(q_2)g_{cdba}(q_1)] f_\epsilon(q_2, q_1) f_\epsilon(q_1, q_2) \tag{2.29}$$

and

$$\langle S_\epsilon^{(4)} \rangle_X = \frac{1}{\pi^4} \int_{-\infty}^\infty dq_2 \int_{-\infty}^\infty dq_1 \sum_{c,d} [g_{adcb}(q_2)g_{bcda}(q_1) - g_{adca}(q_2)g_{bcdb}(q_1)] f_\epsilon^2(q_2, q_1), \tag{2.30}$$

where the sum over c and d is restricted to magnetic substates of the $1s$ state, and where

$$\begin{aligned} f_\epsilon(q_2, q_1) &= \int_{-\infty}^\infty dz \frac{1}{E_0 - z(1 + i\delta)} \frac{\epsilon}{\epsilon^2 + (E_0 - z - q_2)^2} \frac{\epsilon}{\epsilon^2 + (E_0 - z + q_1)^2} \\ &= \frac{-\pi\epsilon}{(q_2 + q_1)^2 + 4\epsilon^2} \frac{q_2 - q_1 - 4i\epsilon}{(q_2 - i\epsilon)(q_1 + i\epsilon)} . \end{aligned} \tag{2.31}$$

To isolate the singularity, we write

$$f_\epsilon(q_2,q_1)f_\epsilon(q_1,q_2) = \tfrac{1}{2}[f_\epsilon(q_2,q_1)+f_\epsilon(q_1,q_2)]^2 - \tfrac{1}{2}[f_\epsilon^2(q_2,q_1)+f_\epsilon^2(q_1,q_2)]. \tag{2.32}$$

The term proportional to

$$\tfrac{1}{2}[f_\epsilon(q_2,q_1)+f_\epsilon(q_1,q_2)]^2 = \frac{-2\pi^2\epsilon^4}{(q_2^2+\epsilon^2)^2(q_1^2+\epsilon^2)^2} \tag{2.33}$$

in Eq. (2.29) completely cancels the term proportional to $\langle S_\epsilon^{(2)}\rangle^2$ in Eq. (2.1), by virtue of the identity

$$\sum_{c,d}[g_{abcd}(q_2)g_{cdab}(q_1) - g_{abcd}(q_2)g_{cdba}(q_1)] = [g_{abab}(q_2) - g_{abba}(q_2)][g_{abab}(q_1) - g_{abba}(q_1)]. \tag{2.34}$$

The net degenerate-intermediate-state (D) contribution is then $\Delta E_D = \Delta E_{DL} + \Delta E_{DX}$, where

$$\Delta E_{DL} = \lim_{\epsilon\to 0}\frac{2i\epsilon}{\pi^4}\int_{-\infty}^{\infty}dq_2\int_{-\infty}^{\infty}dq_1\sum_{c,d}[g_{abcd}(q_2)g_{cdba}(q_1) - g_{abcd}(q_2)g_{cdab}(q_1)]f_\epsilon^2(q_2,q_1)\,, \tag{2.35}$$

and

$$\Delta E_{DX} = \lim_{\epsilon\to 0}\frac{2i\epsilon}{\pi^4}\int_{-\infty}^{\infty}dq_2\int_{-\infty}^{\infty}dq_1\sum_{c,d}[g_{adcb}(q_2)g_{bcda}(q_1) - g_{adca}(q_2)g_{bcdb}(q_1)]f_\epsilon^2(q_2,q_1)\,, \tag{2.36}$$

where we have used the facts that $f_\epsilon(q_1,q_2) = f_\epsilon(-q_2,-q_1)$ and $g_{abcd}(-q) = g_{abcd}(q)$.

These expressions contain integrals over q_2 and q_1 of the form

$$I_\epsilon = \int_{-\infty}^{\infty}dq_2\int_{-\infty}^{\infty}dq_1\,h(q_2,q_1)f_\epsilon^2(q_2,q_1)\,, \tag{2.37}$$

where $h(q_2,q_1)$ is some function of q_2 and q_1. The main contribution to such an integral comes from the region where $q_2 \approx -q_1$, so we replace $h(q_2,q_1)$ in (2.37) by $h(q_2,-q_2)$,

$$I_\epsilon = \int_{-\infty}^{\infty}dq_2\int_{-\infty}^{\infty}dq_1\,h(q_2,-q_2)f_\epsilon^2(q_2,q_1) + \cdots$$

$$= \frac{\pi^3}{4\epsilon}\int_{-\infty}^{\infty}dz\,h(z,-z)\frac{z-5i\epsilon}{(z-3i\epsilon)(z-i\epsilon)^2} + \cdots, \tag{2.38}$$

where the dots represent terms of higher order in ϵ. The validity of the above replacement in the present context was checked by a lengthy independent calculation that does not make this approximation. Substituting (2.38) into (2.35) and (2.36), we obtain

$$\Delta E_{DL} = \lim_{\epsilon\to 0+}\frac{-i}{4\pi}\sum_{a,b,c,d}\int dz\,g_{abcd}(z)\tilde{g}_{cdab}(z)\frac{z-5i\epsilon}{(z-3i\epsilon)(z-i\epsilon)^2}\,, \tag{2.39}$$

and

$$\Delta E_{DX} = \lim_{\epsilon\to 0+}\frac{i}{4\pi}\sum_{a,b,c,d}\int dz\,[g_{adcb}(z)g_{bcda}(z) - g_{adca}(z)g_{bcdb}(z)]\frac{z-5i\epsilon}{(z-3i\epsilon)(z-i\epsilon)^2}\,. \tag{2.40}$$

These two expressions are valid in any gauge with the appropriate gauge-dependent definition of the g_{ijkl} factors. Were it not for the branch cuts in the photon propagator, (2.39) and (2.40) would vanish because the poles are on the same side of the axis. However, the presence of the cuts leads to nonvanishing contributions to the energy.

In Feynman gauge, we perform the z integrals in (2.39) and (2.40) analytically, finding that ΔE_{DL} and ΔE_{DX} each diverge logarithmically as $\epsilon \to 0+$. However, the divergent part cancels identically between the two leaving a finite sum in the limit $\epsilon \to 0+$

$$\Delta E_D = \frac{\alpha^2}{2\pi} \sum_{a,b,c,d} \int d^3x_1 d^3x_2 d^3x_3 d^3x_4 \, \ln(x_{12} + x_{34}) \left(\frac{1}{x_{12}} + \frac{1}{x_{34}} \right)$$
$$\times \Big\{ \phi_a^\dagger(\mathbf{x}_1) \alpha_\mu \phi_c(\mathbf{x}_1) \phi_b^\dagger(\mathbf{x}_2) \alpha^\mu \phi_d(\mathbf{x}_2)$$
$$\times \left[\phi_c^\dagger(\mathbf{x}_3) \alpha_\nu \phi_b(\mathbf{x}_3) \phi_d^\dagger(\mathbf{x}_4) \alpha^\nu \phi_a(\mathbf{x}_4) - \phi_c^\dagger(\mathbf{x}_3) \alpha_\nu \phi_a(\mathbf{x}_3) \phi_d^\dagger(\mathbf{x}_4) \alpha^\nu \phi_b(\mathbf{x}_4) \right]$$
$$+ \Big[\phi_a^\dagger(\mathbf{x}_1) \alpha_\mu \phi_c(\mathbf{x}_1) \phi_d^\dagger(\mathbf{x}_2) \alpha^\mu \phi_b(\mathbf{x}_2) \phi_b^\dagger(\mathbf{x}_3) \alpha_\nu \phi_d(\mathbf{x}_3) \phi_c^\dagger(\mathbf{x}_4) \alpha^\nu \phi_a(\mathbf{x}_4)$$
$$- \phi_a^\dagger(\mathbf{x}_1) \alpha_\mu \phi_c(\mathbf{x}_1) \phi_d^\dagger(\mathbf{x}_2) \alpha^\mu \phi_a(\mathbf{x}_2) \phi_b^\dagger(\mathbf{x}_3) \alpha_\nu \phi_d(\mathbf{x}_3) \phi_c^\dagger(\mathbf{x}_4) \alpha^\nu \phi_b(\mathbf{x}_4) \Big] \Big\} . \quad (2.41)$$

Only the spatial indices $\mu, \nu = 1$–3 give a nonvanishing contribution.

III. NUMERICAL EVALUATION

The numerical calculation was carried out as follows. Firstly, the sum over magnetic substates was carried out analytically using standard Racah algebra, reducing the sum over a, b, m, and n to sums over the allowed angular quantum numbers of the intermediate states m and n and sums over their principal quantum numbers n_m and n_n. These latter sums include both positive- and negative-energy states. Additionally, there is a sum over the multipolarities of each of the two g_{ijkl} factors. One of these sums (over l, say) is infinite, while the other is finite, constrained by triangular conditions for a fixed value of l. This situation is analogous to the MBPT treatment of He in Ref. [1]. We refer to the infinite sum over l as the "partial-wave" expansion of the terms.

The sum over principal quantum numbers was done with a relativistic finite basis set constructed from B splines [21], incorporating at least 70 positive- and 70 negative-energy states per angular quantum number to ensure adequate saturation of the sums. The ω integral was performed to high numerical accuracy for each partial wave by a Gaussian integration method. The infinite partial-wave sum, which was the outermost "loop" in the calculation, was truncated at $l = 8$ and extrapolated to infinity by fitting to polynomials in $1/l$. The finite size of the nucleus is included by using a Fermi distribution for the nuclear charge with parameters given in Ref. [22]. The calculation was checked by two independent codings, and by varying the details of the procedure, for example, by performing the partial-wave sum before the ω integration. The leading numerical error in the final tabulations arises principally from a combination of basis-set truncation error and error in the partial-wave extrapolation. We estimate the total numerical error to be less than 0.000 03 a.u. for $Z = 70$–110, less than 0.000 02 a.u. for $Z = 40$–60, less than 0.000 01 a.u. for $Z = 20$ and 30, and less than 0.0000 03 a.u. for $Z = 10$.

The ground-state term ΔE_D was evaluated several different ways. In one, we computed (2.41) with Monte Carlo techniques. As a variant, we included the z integration in the Monte Carlo procedure and worked directly from the sum of the expressions (2.39) and (2.40). We also considered an *ad hoc* regularization of the expressions (2.39) and (2.40) in which we replaced z in the rational function by $z + \Delta$, with Δ real, and let $\epsilon \to 0+$. This effectively modifies the eigenvalue of the intermediate $1s$ states. The resulting expressions were evaluated by a contour rotation and extrapolated to $\Delta \to 0$, giving identical numerical results for ΔE_D to those obtained with the previous methods.

The entire calculation was checked further by performing it in both the Coulomb and Feynman gauges. Table I gives a breakup of the calculation in each gauge for two Z values. Here, $\Delta E^+_{\rm pole}$ and $\Delta E^-_{\rm pole}$ are the parts of the pole term $\Delta E^{\rm pole}_L + \Delta E^{\rm pole}_X$ [Eqs. (2.25) and (2.26)] where m is a positive- or negative-energy state, respectively. The contour term $\Delta E_{CL} + \Delta E_{CX}$

TABLE I. Ladder plus crossed-ladder diagrams calculated in the Feynman and Coulomb gauges for two Z values. See text for explanation of symbols. Units are a.u.

	$Z = 10$ ($\Delta E_{\rm MBPT} = -0.160999$)		$Z = 80$ ($\Delta E_{\rm MBPT} = -0.40792$)	
Term	Feynman	Coulomb	Feynman	Coulomb
$\Delta E^+_{\rm pole}$	−0.112776	−0.112776	−0.25371	−0.25371
$\Delta E^-_{\rm pole}$	0.000000	0.000000	−0.00065	−0.00065
ΔE^{++}	−0.048061	−0.048088	−0.12633	−0.12422
ΔE^{+-}	0.000010	−0.000018	0.02346	0.01013
ΔE^{--}	−0.000145	−0.000090	−0.02820	−0.01697
ΔE_C	−0.048196	−0.048196	−0.13107	−0.13106
ΔE_D	(1.16×10^{-7})	(1.16×10^{-7})	0.00415	0.00415
$\Delta E_{\rm QED}$	0.000026	0.000026	0.02664	0.02665
ΔE (total)	−0.160972	−0.160972	−0.38128	−0.38127

TABLE II. Decomposition of the sum of the ladder and crossed-ladder diagrams into contributions from positive- and negative-energy intermediate states. Calculations carried out in the Feynman gauge. Units are a.u.

Z	$\Delta E^{\rm pole}$	ΔE^{++}	ΔE^{+-}	ΔE^{--}	ΔE_D
10	−0.112777	−0.048061	0.000010	−0.000145	0.000000
20	−0.11816	−0.05178	0.00016	−0.00091	0.00000
30	−0.12737	−0.05756	0.00073	−0.00255	0.00003
40	−0.14078	−0.06544	0.00205	−0.00523	0.00012
50	−0.15897	−0.07565	0.00449	−0.00902	0.00037
60	−0.18289	−0.08867	0.00849	−0.01402	0.00094
70	−0.21393	−0.10519	0.01457	−0.02035	0.00208
80	−0.25436	−0.12633	0.02346	−0.02820	0.00415
90	−0.30787	−0.15392	0.03617	−0.03785	0.00769
100	−0.38100	−0.19113	0.05427	−0.04980	0.01346
110	−0.48595	−0.24396	0.08032	−0.06486	0.02255

[Eqs. (2.27) and (2.28)] has been similarly decomposed into contributions where the intermediate states m and n have both positive or both negative energy, ΔE^{++} and ΔE^{--}, and a contribution where one is positive and the other is negative, ΔE^{+-}. The total energy, including the ground-state term ΔE_D, is denoted by ΔE. The term $\Delta E_{\rm QED} = \Delta E - \Delta E_{\rm MBPT}$ is discussed further below. The pole terms $\Delta E^{+}_{\rm pole}$ and $\Delta E^{-}_{\rm pole}$, the total contour term $\Delta E_C = \Delta E^{++} + \Delta E^{+-} + \Delta E^{--}$, and the ground-state term ΔE_D are found to be separately gauge invariant.

Table II gives the analogous breakup at $Z = 10,20,\ldots,$ 110 for the Feynman gauge only, with $\Delta E^{\rm pole}$ the total pole term. As is clear from Table I, the breakup into ΔE^{++}, ΔE^{+-}, and ΔE^{--} is gauge dependent and would be different in the Coulomb gauge. The point we wish to emphasize is the significant role played by the negative-energy states for all Z. The final column in Table II gives ΔE_D. Figure 4 shows this contribution to scale closely as $(Z\alpha)^5$. For low Z, we find $\Delta E_D \approx 0.056\,(Z\alpha)^5$ a.u..

Now, as discussed in the Introduction, it is desirable to combine this calculation with high-accuracy MBPT calculations. To do this, in the second, third, and fourth columns of Table III, we also present the three second-order contributions from MBPT mentioned above, $E^{(2)}$, $B^{(2)}$, and B-B. In the last column of Table III, we give the difference between the QED and MBPT results, which we refer to as the "residual QED correction" $\Delta E_{\rm QED}$. This correction must be added to the MBPT calculation to account for the omitted negative-energy and retardation contributions, and the crossed-ladder diagram.

We analyze $\Delta E_{\rm QED}$ further in Table IV, where for two Z values we give the terms arising from two Coulomb photons, from one Coulomb and one transverse photon, and from two transverse photons, in a Coulomb-gauge calculation. An exact QED evaluation is compared with the corresponding MBPT values. In fractional terms the two-transverse-photon term is most modified, but in absolute terms all combinations make significant contributions to $\Delta E_{\rm QED}$.

In the Coulomb gauge, the two-Coulomb-photon term makes no contribution to ΔE_D because of the absence of branch cuts in the photon propagator. We find further that the one-transverse–one-Coulomb term cancels identically between the ladder and crossed-ladder diagrams, so that ΔE_D arises entirely from the transverse-transverse term. Furthermore, in the Coulomb gauge,

TABLE III. The present calculation ΔE is compared with a second-order MBPT calculation $E^{(2)} + B^{(2)}$+B-B to determine the residual QED correction $\Delta E_{\rm QED}$. Units are a.u.

Z	ΔE	$E^{(2)}$	$B^{(2)}$	B-B	$\Delta E_{\rm QED}$
10	−0.160972	−0.158083	−0.002870	−0.000046	0.000026
20	−0.17069	−0.15952	−0.01095	−0.00043	0.00021
30	−0.18673	−0.16226	−0.02363	−0.00163	0.00078
40	−0.20927	−0.16662	−0.04059	−0.00415	0.00208
50	−0.23878	−0.17303	−0.06179	−0.00854	0.00458
60	−0.27614	−0.18211	−0.08750	−0.01542	0.00889
70	−0.32283	−0.19482	−0.11841	−0.02545	0.01585
80	−0.38128	−0.21271	−0.15578	−0.03943	0.02664
90	−0.45579	−0.23844	−0.20185	−0.05846	0.04296
100	−0.55420	−0.27690	−0.26061	−0.08414	0.06744
110	−0.69190	−0.33769	−0.33947	−0.11913	0.10439

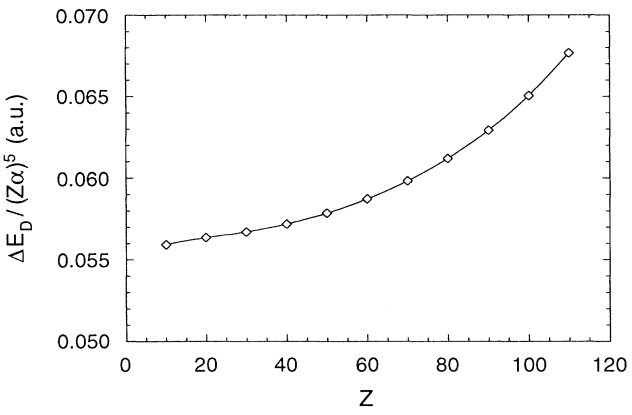

FIG. 4. The ground-state term ΔE_D scaled by $(Z\alpha)^5$.

ΔE_{DL} and ΔE_{DX} are each finite as $\epsilon \to 0+$ or $\Delta \to 0+$. For example, at $Z = 80$, $\Delta E_{DL} = 0.032\,71$ a.u. and $\Delta E_{DX} = -0.028\,56$ a.u.. By contrast, in the Feynman gauge, only the sum of these terms is finite.

IV. ANALYSIS AND CONCLUSIONS

The principal result of this paper is the tabulation of $\Delta E_{\rm QED}$ given in the last column of Table III. It is this quantity that is to be added to MBPT or configuration-interaction (CI) calculations of the ground states of heliumlike ions using a no-pair Hamiltonian with the instantaneous Breit interaction. When the as yet uncalculated diagrams of Figs. 2(c) and 2(d) are included, the S-matrix approach will have included all the previously determined $(Z\alpha)^3$ a.u. corrections along with a set of $(Z\alpha)^4$ a.u. and higher corrections. It is clearly of interest to isolate these new corrections. To this end, we concentrate on ΔE in the first column of Table III rather than $\Delta E_{\rm QED}$. This is because the MBPT expressions also contain $(Z\alpha)^3$ a.u. and higher-order corrections. In Table V, we show a comparison of ΔE with the known corrections of order $(Z\alpha)^{0,2,3}$, which are [23]

$$\Delta E[(Z\alpha)^0] = -0.157\,666\,38, \tag{4.1}$$

$$\Delta E[(Z\alpha)^2] = -0.6356(Z\alpha)^2, \tag{4.2}$$

and

$$\Delta E[(Z\alpha)^3] = \frac{(Z\alpha)^3}{8\pi}\left(\frac{98}{9} - \frac{8}{3}\ln 2 - \frac{2}{3}\ln\alpha\right) - \frac{14}{3}Q - \frac{2}{3\pi}\alpha^3 M', \tag{4.3}$$

where Q for the ground state in hydrogenic approximation is [23]

$$Q = -\frac{(Z\alpha)^3}{8\pi}(\ln 2Z - 1.333) \tag{4.4}$$

and

$$-\frac{2}{3\pi}\alpha^3 M' = \frac{(Z\alpha)^3}{8\pi}\left(-\frac{16}{3}\ln Z - 1.88\right). \tag{4.5}$$

The term M' is generally combined with another term from the vertex diagram to give the full Bethe logarithm, which has been analyzed in the $1/Z$ expansion by Goldman and Drake [24]. However, M' has not, to our knowledge, been separately computed before. We evaluated it by working in Coulomb gauge and evaluating the one-Coulomb-photon–one-transverse-photon interaction ladder and crossed-ladder diagrams with the same method that leads to the Bethe logarithm. Specifically, this involves taking the transverse photon pole and making the dipole approximation in the integration over the photon energy, which is logarithmically divergent in this approximation, but is cut off at 1 a.u..

It is of interest to compare our inferred QED correction in Table III to the QED corrections calculated by Sucher [9] and Araki [10], so that the part of the present calculation that is truly new, that is of order $(Z\alpha)^4$ a.u.

TABLE IV. Comparison of exact Coulomb-gauge QED calculations with MBPT calculations. C-C, two Coulomb photons; C-B, one Coulomb and one transverse photon; B-B, two transverse photons. The final column is the difference of the second and third columns. Units are a.u.

Term	MBPT	QED	$\Delta E_{\rm QED}$
	$Z = 10$		
C-C	−0.158083	−0.158058	0.000025
C-B	−0.002870	−0.002846	0.000024
B-B	−0.000046	−0.000069	−0.000023
Total	−0.160999	−0.160972	0.000026
	$Z = 80$		
C-C	−0.21271	−0.20556	0.00715
C-B	−0.15578	−0.15905	−0.00327
B-B	−0.03943	−0.01666	0.02277
Total	−0.40792	−0.38127	0.02665

TABLE V. Comparison of full QED calculation with low-order terms from the $(Z\alpha)$ expansion to determine the residual terms of order $(Z\alpha)^4$ and higher. Units are a.u.

Z	ΔE	$(Z\alpha)^0+(Z\alpha)^2$	$(Z\alpha)^3$	$(Z\alpha)^4\cdots$
10	−0.160972	−0.161051	0.000092	−0.000013
20	−0.17069	−0.17120	0.00068	−0.00016
30	−0.18673	−0.18813	0.00217	−0.00077
40	−0.20927	−0.21182	0.00494	−0.00239
50	−0.23878	−0.24228	0.00937	−0.00586
60	−0.27614	−0.27951	0.01578	−0.01241
70	−0.32283	−0.32351	0.02451	−0.02383
80	−0.38128	−0.37428	0.03589	−0.04289
90	−0.45579	−0.43182	0.05021	−0.07418
100	−0.55420	−0.49613	0.06779	−0.12586
110	−0.69190	−0.56721	0.08892	−0.21361

and higher, can be seen. To do this, we have tabulated in the first two columns of Table V our complete calculation and the sum of the $(Z\alpha)^0$ and $(Z\alpha)^2$ contributions. In the third column, we give the known $(Z\alpha)^3$ terms. In the final column, the new physics of order $(Z\alpha)^4$ and higher, calculated here, is given. Writing the terms in the final column as $c(Z)(Z\alpha)^4$, we show a plot of the function $c(Z)$ in Fig. 5. For $Z = 10$–110, $c(Z)$ lies in the range -0.43 ± 0.10 a.u..

We can perform a similar breakup of the QED residue $\Delta E_{\rm QED}$ into "known" terms of order $(Z\alpha)^3$ a.u. and new higher-order terms. To do this, we note that the MBPT calculation contains all of $\Delta E[(Z\alpha)^0]$ and $\Delta E[(Z\alpha)^2]$, and in addition a part $\Delta E_{\rm MB}[(Z\alpha)^3]$ of $\Delta E[(Z\alpha)^3]$, where

$$\Delta E_{\rm MB}[(Z\alpha)^3] = \frac{(Z\alpha)^3}{8\pi}\left(\frac{19}{3}-\frac{\pi}{2}\right). \tag{4.6}$$

Writing the new terms of order $(Z\alpha)^4$ a.u. and higher in $\Delta E_{\rm QED}$ as $d(Z)(Z\alpha)^4$, that is, putting

$$\Delta E_{\rm QED} = \Delta E[(Z\alpha)^3] - \Delta E_{\rm MB}[(Z\alpha)^3] + d(Z)(Z\alpha)^4, \tag{4.7}$$

we plot the function $d(Z)$ in Fig. 6. It lies in the range 0.27 ± 0.03 a.u. for $Z = 10$–110.

In summary, we have applied a contour rotation method that allow us to evaluate the diagrams of Figs. 2(a) and 2(b) numerically. The dominant Coulomb correlation has been picked up along with terms that contribute at the order of fine structure, which are associated with solution of the Dirac-Coulomb-Breit Hamiltonian. Because the method involves an exact QED formulation, additional physics, $\Delta E_{\rm QED}$, enters. This physics, which enters at the level of $1/Z$ of the Lamb shift, is an important part of any calculation seeking to test our understanding of radiative corrections in high-Z few electron atoms. The next steps are to extend the calculation to the intensively studied $n = 2$ energy levels of the helium isoelectronic sequence, and to begin the study of

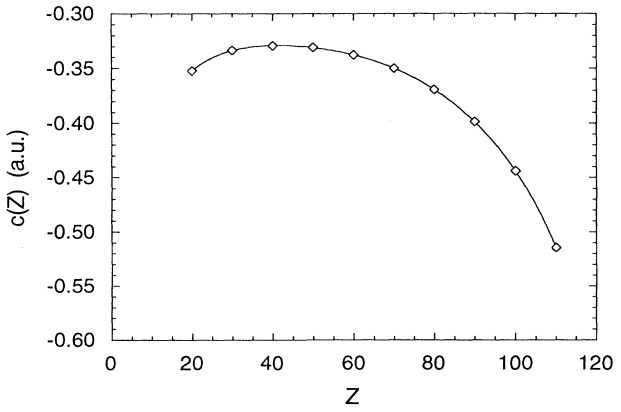

FIG. 5. The function $c(Z)$ such that terms of order $(Z\alpha)^4$ a.u. and higher in ΔE are given by $c(Z)(Z\alpha)^4$.

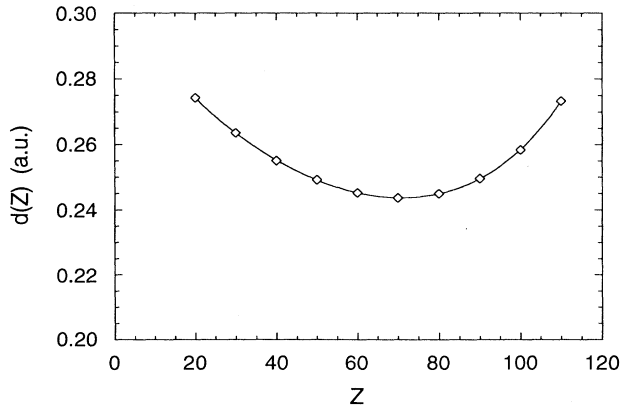

FIG. 6. The function $d(Z)$ such that terms of order $(Z\alpha)^4$ a.u. and higher in $\Delta E_{\rm QED}$ are given by $d(Z)(Z\alpha)^4$.

the other class of diagrams that contribute at this same level, those involving one radiative correction and one photon exchange shown in Fig. 2(c).

Note added in proof. It has been brought to our attention that Eq. (2.41) has been derived with a method based on Rayleigh-Schrödinger perturbation theory by V. M. Shabaev [Sov. Phys. J. **33**, 660 (1990)]. We have obtained the analytic result $E_D = (37/210\pi)(Z\alpha)^5$ a.u. for that quantity in agreement with the numerical fit in Sec. III.

ACKNOWLEDGMENTS

This work was partially supported by NSF Grant No. PHY-92-04089. We would like to thank G. W. F. Drake, E. Lindroth, J. Morgan, and D. Yennie for valuable conversations. P.J.M. and J.S. would like to thank the Institute for Nuclear Theory at the University of Washington for its hospitality and the Department of Energy for partial support during the completion of this work.

[1] W.R. Johnson and J. Sapirstein, Phys. Rev. A **46**, R2197 (1992).
[2] W.R. Johnson, S.A. Blundell, and J. Sapirstein, Phys. Rev. A **37**, 2764 (1988); **38**, 2699 (1988); **42**, 1087 (1990).
[3] J. Sucher, Phys. Rev. A **30**, 703 (1980).
[4] G.E. Brown and G. Ravenhall, Proc. R. Soc. London Ser. A **208**, 552 (1951).
[5] G. Breit, Phys. Rev. **34**, 553 (1929).
[6] M. Mittleman, Phys. Rev. A **5**, 2395 (1971).
[7] (a) B. Zygelman and M.H. Mittleman, J. Phys. B **19**, 1891 (1986); (b) B. Zygelman, in *Relativistic, Quantum Electrodynamic and Weak Interaction Effects in Atoms*, Proceedings of a Program held at the Institute for Theoretical Physics at Santa Barbara, CA, 1988, edited by Walter Johnson, Peter Mohr, and Joseph Sucher, AIP Conf. Proc. No. 189 (AIP, New York, 1989), p. 408.
[8] H.A. Bethe and E.E. Salpeter, Phys. Rev. **82**, 309 (1951); E.E. Salpeter and H.A. Bethe, *ibid.* **84**, 1232 (1951); J. Schwinger, Proc. Natl. Acad. Sci. U.S.A **37**, 452 (1951); **37**, 455 (1951).
[9] J. Sucher, Phys. Rev. **109**, 1010 (1958).
[10] H. Araki, Prog. Theor. Phys. Jpn. **17**, 619 (1957).
[11] P.K. Kabir and E.E. Salpeter, Phys. Rev. **108**, 1256 (1957).
[12] M. Douglas and N.M. Kroll, Ann. Phys. (N.Y.) **82**, 89 (1974).
[13] P.J. Mohr, Phys. Rev. A **32**, 1949 (1985); L.N. Labzovskii, Zh. Eksp. Teor. Fiz. **59**, 168 (1970) [Sov. Phys. JETP **32**, 94 (1970); L.N. Ivanov, E.P. Ivanova, and U.I. Safronova, J. Quant. Spectrosc. Radiat. Trans. **15**, 553 (1975).
[14] M. Gell-Mann and F. Low, Phys. Rev. **84**, 350 (1951).
[15] J. Sucher, Phys. Rev. **107**, 1448 (1957).
[16] H.T. Doyle, *Advances in Atomic and Molecular Physics* (Academic, New York, 1969), Vol. 5, p. 337.
[17] See the Proceedings of the Nobel Symposium on Highly Charged Ions, Saltsjobaden, Sweden, 1992 [Phys. Scr. **T46** (1993)].
[18] M. Chen, K.T. Cheng, and W.R. Johnson, Phys. Rev. A **47**, 3692 (1993).
[19] J. Sapirstein, in Ref. [7(b)], p. 196.
[20] P. J. Mohr, in Ref. [7(b)], p. 47.
[21] W.R. Johnson, S.A. Blundell, and J. Sapirstein, Phys. Rev. A **37**, 307 (1988).
[22] W.R. Johnson and G. Soff, At. Data. Nucl. Data Tables **33**, 405 (1985).
[23] G.W.F. Drake, Can. J. Phys. **66**, 586 (1988).
[24] S.P. Goldman and G.W.F. Drake, J. Phys. B **17**, L197 (1984).